Ultrasonic breast imaging using a wave-equation migration method

Lianjie Huang[a], Nebojsa Duric[b], and Peter Littrup[c]

[a]Mail Stop D443, Los Alamos National Laboratory, Los Alamos, NM 87545

[b]Department of Physics and Astronomy, University of New Mexico, Albuquerque, NM 87131

[c]Karmanos Cancer Institute, 110 East Warren Avenue, Detroit, MI 48201

ABSTRACT

Reflection imaging has the potential to produce higher-resolution breast images than transmission tomography; however, the current clinical reflection imaging technique yields poor-quality breast images due to speckle. We present a new ultrasonic breast imaging method for obtaining high-resolution and clear breast images using ultrasonic reflection data acquired by a new ultrasonic scanning device that provides a better illumination of targets of interest than the clinical B-scan. The new imaging method is based on the solution of the wave equation in Cartesian coordinates and is implemented using Fast Fourier Transform algorithms. We apply the new ultrasonic breast imaging method to two ultrasonic data sets obtained using an experimental ultrasound scanner recently developed by the Karmanos Cancer Institute. One data set was acquired for a "cyst" phantom using 360 transmitter positions and 321 receiver positions along a 20-cm diameter ring. Another data set was collected with 180 transmitter positions and 1601 receiver positions along a 30-cm diameter ring with the breast specimen located at the center of the ring. We report on the breast imaging results for these two data sets using the new breast imaging method. The results demonstrate that the wave-equation-based ultrasonic breast imaging has the potential to produce high-resolution breast images.

Keywords: acoustic impedance, breast cancer, ultrasonic breast imaging, wave equation.

1. INTRODUCTION

Breast cancer is the second-leading cause of cancer death for American women. It is the most commonly diagnosed cancer among women, accounting for nearly one of every three cancers diagnosed in women. Early detection is the key to reducing breast-cancer mortality. X-ray mammography that started in 1960's is the only routine screening tool available today, but its effectiveness is now being debated. For instance, some recent studies have shown that x-ray mammography does not reduce breast-cancer mortality.[1,2] Without question, there is an urgent need to develop new and better (more effective) tools for breast-cancer screening and diagnosis. As an alternative to x-ray mammography, ultrasonic breast imaging is one of the most promising screening tools.[3,4] Recent clinical studies have shown that ultrasonic breast imaging has the potential to detect small, early-stage cancers that are missed by x-ray mammography, particularly in younger women with denser breast tissue.[5,6] It has been used for distinguishing between benign and malignant lesions.[4,7] Unfortunately, current ultrasonic breast imaging produces poor-quality images, which greatly limit its capability for cancer detection.[4] Therefore, the United States Food and Drug Administration has approved that ultrasound be used only as an adjunct procedure after initial detection of cancers by mammography.[8]

To improve the capability of ultrasonic breast imaging, the Karmanos Cancer Institute (KCI) is developing a new ultrasound device capable of recording all wavefields including reflected, transmitted, and diffracted ultrasonic waves from breast tissue.[9,10] The recently developed KCI engineering prototypic device has been used to perform a series of experiments for several phantoms and a cadaveric breast specimen to verify the feasibility and capability of the device. The new device collects ultrasonic data in a way that is fundamentally different from the conventional B-mode breast ultrasound, and consequently, a new class of ultrasonic imaging methods that are different from conventional ultrasonic breast imaging methods have to be developed and implemented.[10,11] Previous imaging studies for the data collected using this new prototypic device have been focused on transmission tomography,[11,12] diffraction tomography,[13] and ray-based reflection imaging.[11] Transmission and diffraction tomographic-imaging methods yield images of sound speeds of breast tissue using transmitted and diffracted ultrasonic waves, respectively, whereas reflection imaging produces images of

Medical Imaging 2003: Ultrasonic Imaging and Signal Processing,
William F. Walker, Michael F. Insana, Editors, Proceedings of SPIE
Vol. 5035 (2003) © 2003 SPIE · 1605-7422/03/$15.00

locations where changes of acoustic impedance occur within the breast. The latter could produce higher-resolution breast images than the former.

In this paper, we will introduce a new ultrasonic breast imaging method based on the solution of the wave equation in a constant-velocity medium. We will apply this reflection imaging method to two ultrasonic data sets provided by the Karmanos Cancer Institute. One data set was obtained from scanning a “cyst” phantom containing two “cysts,” and another was from scanning a normal cadaveric breast specimen, both using the KCI engineering prototype of ultrasonic breast-scanning device. We will present the preliminary imaging results for these two data sets using the new imaging method to demonstrate the capability of the proposed method for producing high-resolution breast images. The new KCI ultrasonic breast-scanning device coupled with new imaging algorithms has great potential to provide an effective and essential new screening tool for breast cancer to reduce mortality.

2. METHOD

Ultrasonic-wave propagation in breast tissue is governed by the acoustic-wave equation. For a constant velocity medium in Cartesian coordinates, the solution of the wave equation in the frequency-wavenumber domain can be written as a multiplication of an initial wavefield term with a phase-shift term. We use this solution to “back-propagate” the recorded ultrasonic reflection data from observation positions into locations (breast tissue) from where the ultrasonic waves were reflected. The procedures of ultrasonic breast imaging using the above wave-equation solution is described in the following:

1. Fourier transforming recorded ultrasonic reflection data from the time domain to the frequency domain;
2. Fourier transforming the data from the frequency-space domain to the frequency-wavenumber domain;
3. Multiplying the initial (recorded or extrapolated) wavefield with a phase-shift term to numerically inward “propagating” the wavefield from the receiver/transmitter positions into the target regions (breast specimen);
4. Inverse Fourier transforming the wavefield from the frequency-wavenumber domain into the frequency-space domain to obtain the breast images;
5. Repeating procedures (2)–(4) until the images of all target regions are produced.

Fast Fourier Transform algorithms can be used for the above Fourier transforms during numerical implementation.

In the above wave-equation-based ultrasonic migration imaging method, a frequency range of interest can be selected for imaging, and the effects of ultrasonic-wave attenuation in breast tissue could be approximately compensated during imaging to produce more realistic breast images.

3. EXPERIMENTAL SETUP

The Karmanos Cancer Institute (KCI) recently contracted with Lawrence Livermore National Laboratory to build an engineering prototype capable of acquiring 3-D ultrasonic data (Figure 1). Two ultrasonic reflection data sets were provided by the KCI who acquired them by scanning a “cyst” phantom and a normal cadaveric breast using KCI’s engineering prototypic scanner. The “cyst” phantom consisted of a 4-cm diameter cylinder containing the homogeneous agar and two smaller cylinders that were embedded in the agar and separated from each other. Each small cylinder with a diameter of 1 cm contained a water-alcohol mixture with a lower sound speed than the surrounding agar to mimic the slower sound speed for a fluid filled cyst in a low contrast setting. In another ultrasonic scanning experiment, the normal cadaveric breast specimen was placed in formalin and sealed in a 10-cm diameter, cylindrical container.

In both experiments, the containers were placed in a water tank (see Figure 1) and scanned using KCI’s engineering prototype of ultrasonic scanner at a frequency of 1.5 MHz using 2 microsecond pulses. The transmitted pulse in the background medium surrounding the cylindrical containers and the spectrum of the pulse are shown in Figure 2(a) and (b), respectively. The relatively low frequency of 1.5 MHz was used during the experiments in order to obtain better penetration of ultrasound through the phantom and the dehydrated, formalin-fixed breast. For *in-vivo* breast imaging applications, a higher frequency may be used to further improve imaging resolution because of less ultrasonic-wave attenuation in the human breast compared with the formalin-fixed breast specimen.

The receivers and transmitters were located along a ring trajectory having a diameter of 20 cm for the “cyst” phantom and a diameter of 30 cm when scanning the breast specimen. During the experiments, each cylindrical container was placed at the center of the ring with the long axis of the cylinder oriented vertically relative to the plane of the ring. A total

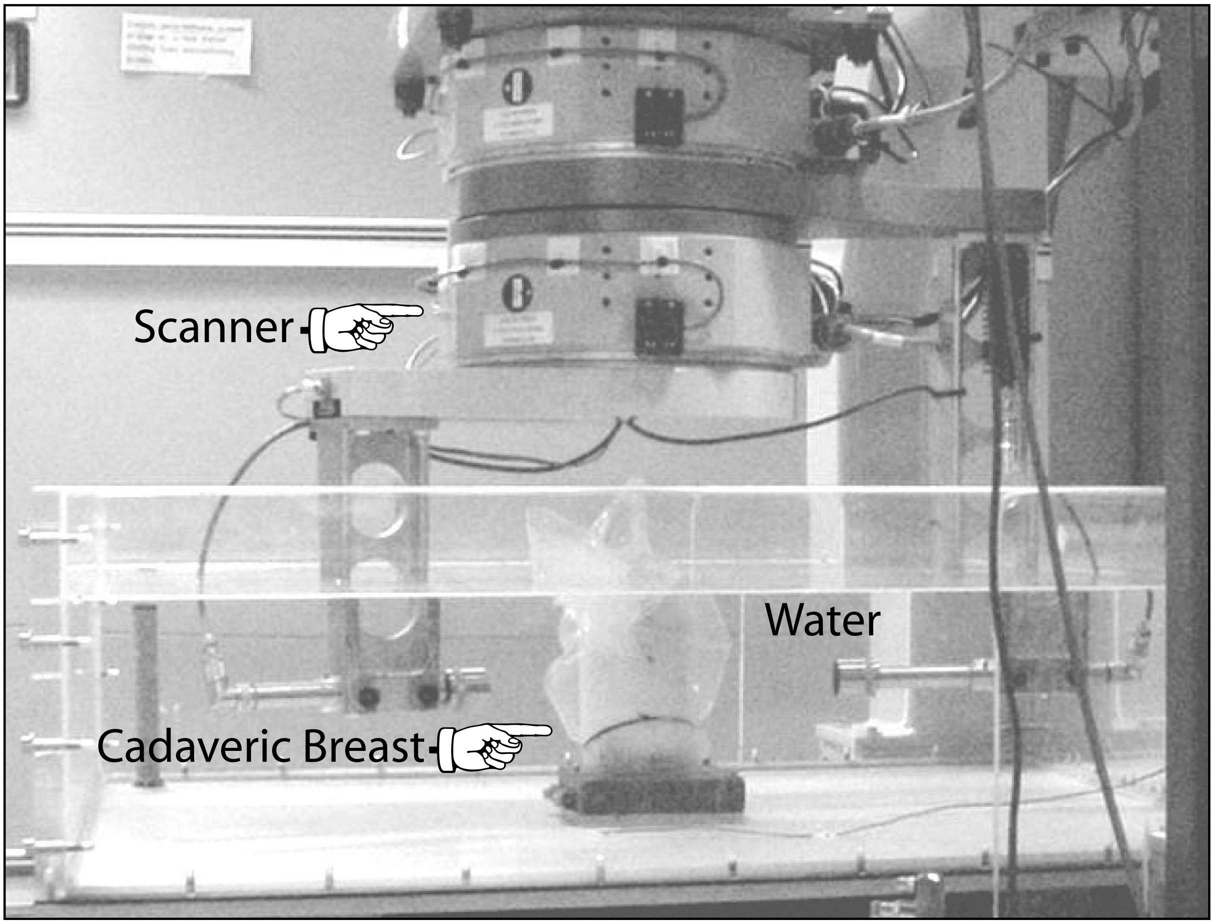

Figure 1. Experimental setup of the KCI engineering prototype of ultrasonic scanner. The breast specimen was placed in the water tank and scanned by the ultrasound.

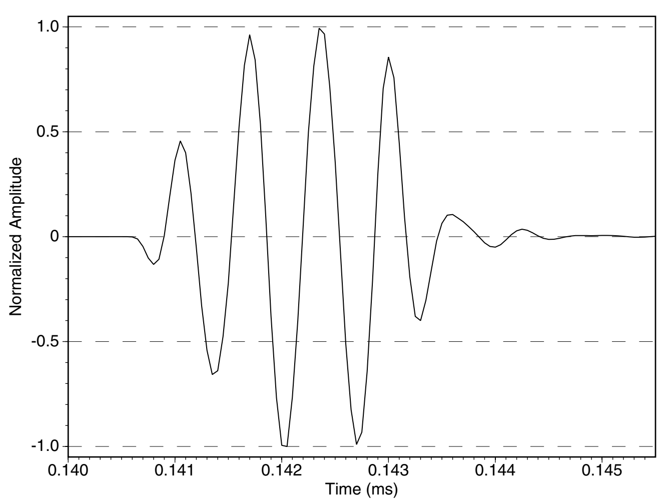

(a) Transmitted pulse

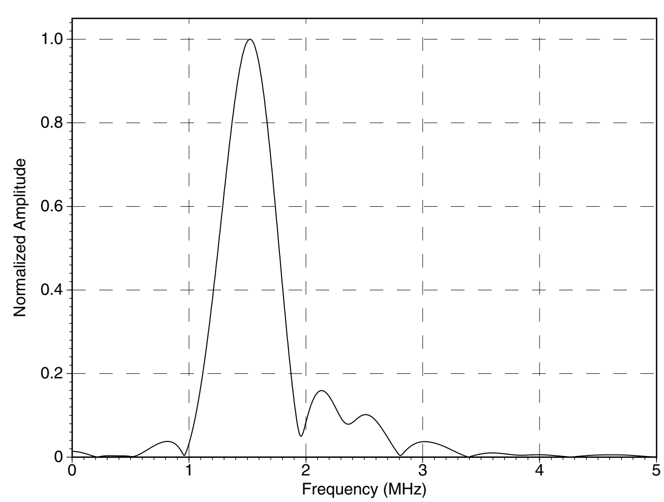

(b) Spectrum

Figure 2. Transmitted pulse of ultrasound (a) and its spectrum (b) in the background medium surrounding the cylindrical containers.

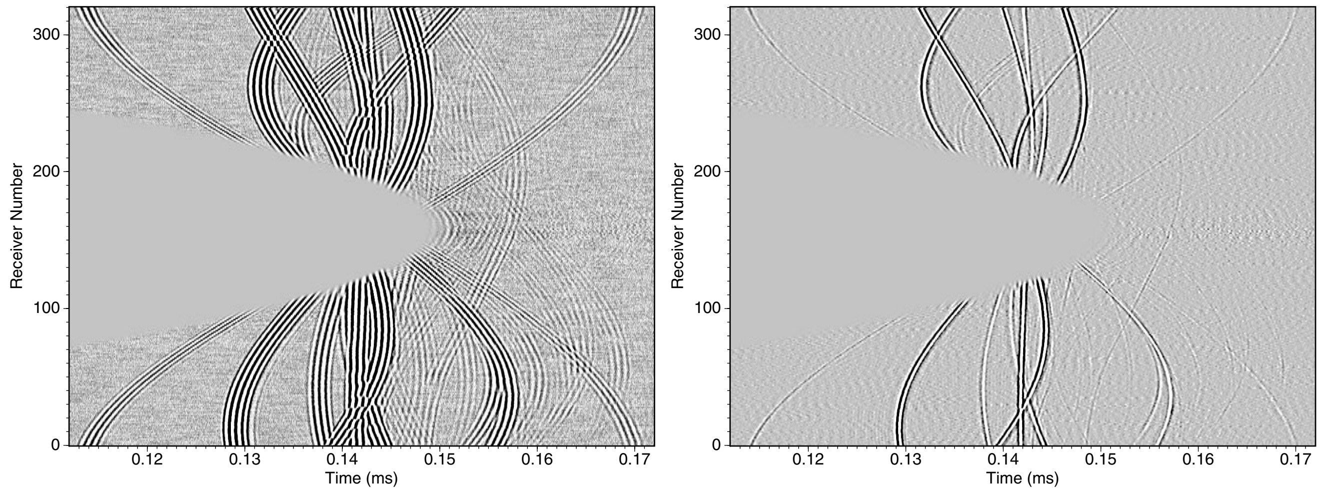

(a) Recorded ultrasonic signals

(b) Deconvolved ultrasonic signals

Figure 3. Recorded ultrasonic signals (a) and those after deconvolution (b) for the "cyst" phantom.

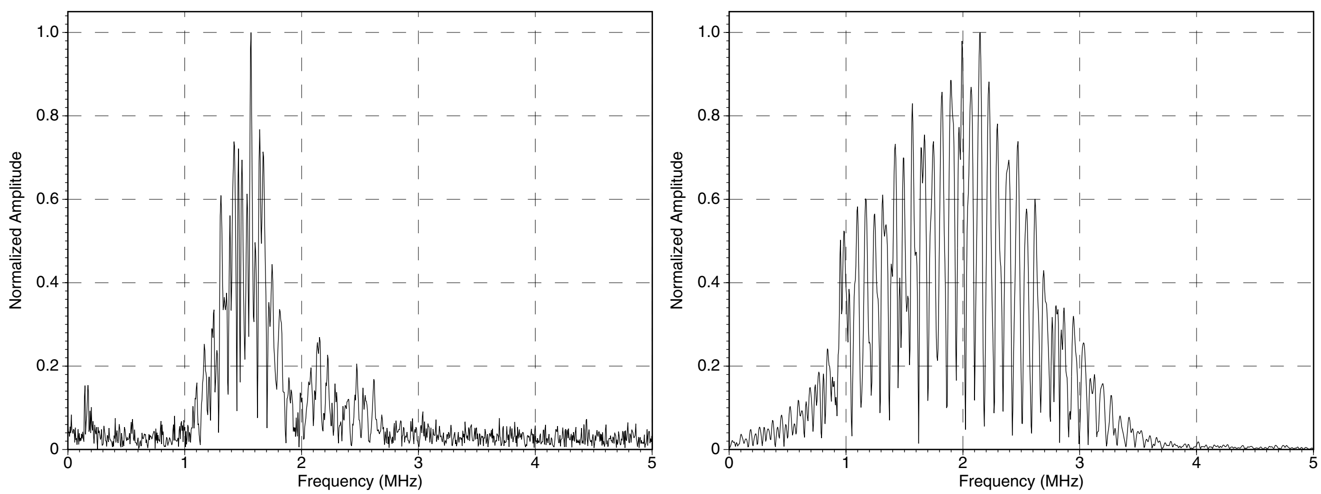

(a) Spectrum of reflection signals

(b) Spectrum of deconvolved reflection signals

Figure 4. Spectra of ultrasonic reflection signals (a) and of those after deconvolution (b) for the "cyst" phantom.

of 360 transmitter positions and 321 receiver positions were used when scanning the "cyst" phantom, and a total of 180 transmitter positions and 1601 receiver positions were used when scanning the breast specimen. Each scan was performed at a slice of 10-mm thickness.

4. IMAGING RESULTS

The recorded ultrasonic data need to be preprocessed before using them for imaging. Figure 3(a) is an example of ultrasonic signals recorded when scanning the "cyst" phantom. Each reflection event shown in Figure 3(a) contains multiple pulses as those plotted in Figure 2(a). Before applying the wave-based ultrasonic migration imaging algorithm to the recorded ultrasonic data, we deconvolved these data with the multiple pulses in Figure 2(a) and then bandpass-filtered them, resulting in signals containing much shorter pulses as displayed in Figure 3(b) compared with those in Figure 3(a). Figures 4(a) and (b) are the corresponding spectra of ultrasonic reflection signals in Figures 3(a) and (b), respectively. Figure 5(a) is the image obtained by applying the proposed wave-based ultrasonic migration imaging to the deconvolved signals (Figure 3b). The acoustic impedance of the "cysts" are different from the surrounding agar, and hence, the ultrasonic

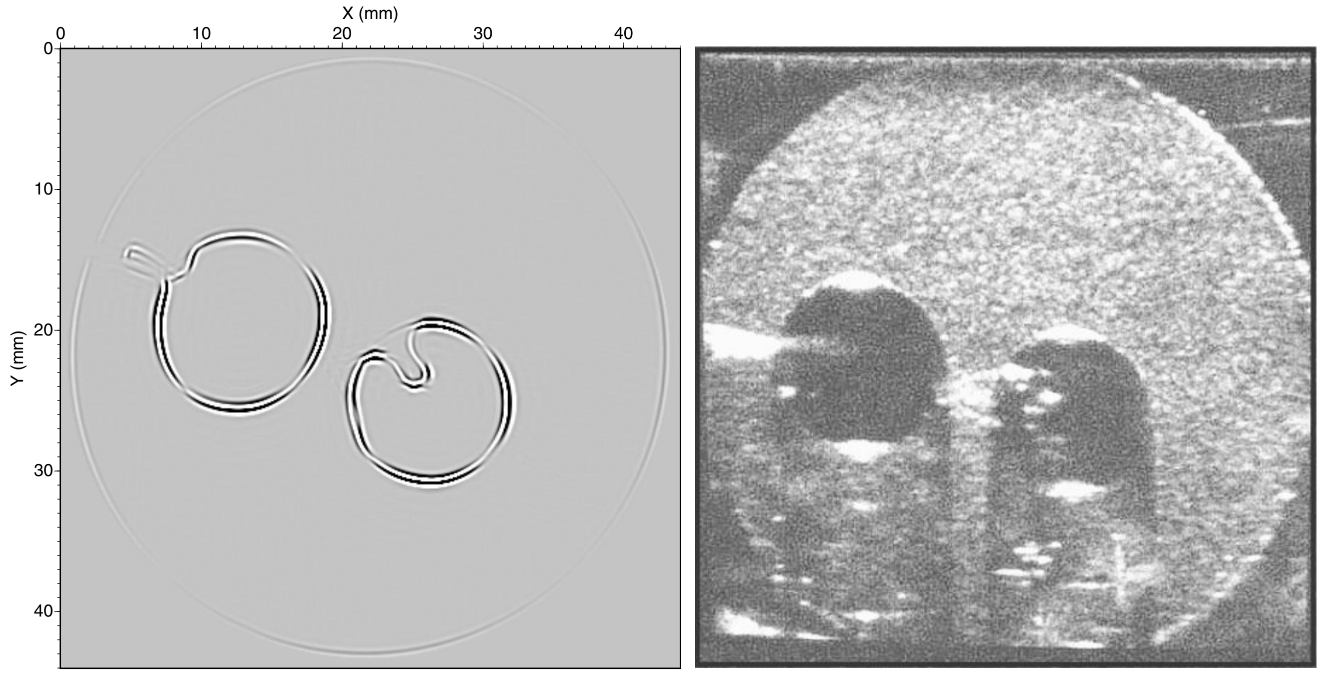

(a) Wave-equation migration image (1.5MHz)

(b) Clinical B-scan image (6-11MHz)

Figure 5. Images obtained using wave-based reflection imaging (a) and medical B-scan (b) for the "cyst" phantom.

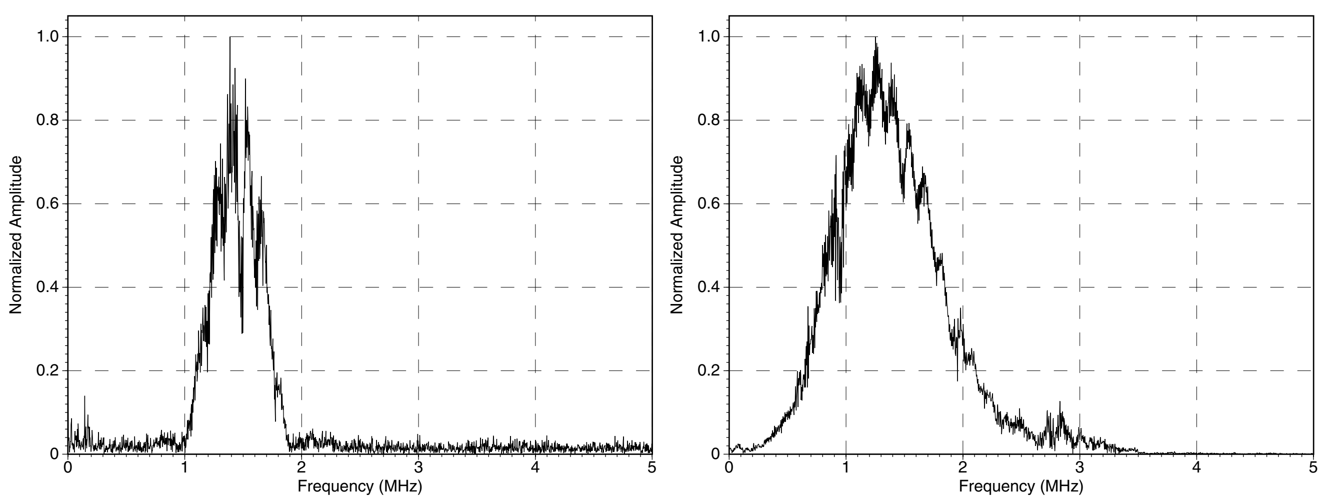

(a) Spectrum of reflected signals

(b) Spectrum of reflected signals after deconvolution

Figure 6. Spectra of reflected ultrasonic waves (a) and those after deconvolution (b) for the breast specimen.

migration imaging clearly shows the shapes of two "cysts" as shown in Figure 5(a). For comparison, the "cyst" phantom was also scanned with a clinical reflection ultrasound unit operating in a frequency range of 6-11 MHz (GE Logiq 600) and the resulting B-scan image is shown in Figure 5(b).[10] We can see that the wave-based ultrasonic imaging result (Figure 5a) gives more detailed structures of the shapes of the "cysts" than the clinical B-scan imaging (Figure 5b), even though the data we used were obtained by the KCI scanner operating in a much lower frequency (1.5 MHz) than that used in the clinical B-scan (6-11 MHz).

We applied the same data preprocessing schemes to ultrasonic reflection data obtained by scanning the breast specimen. The spectra of signals before and after deconvolution are shown in Figures 6(a) and (b). Figure 7 is the image of the breast

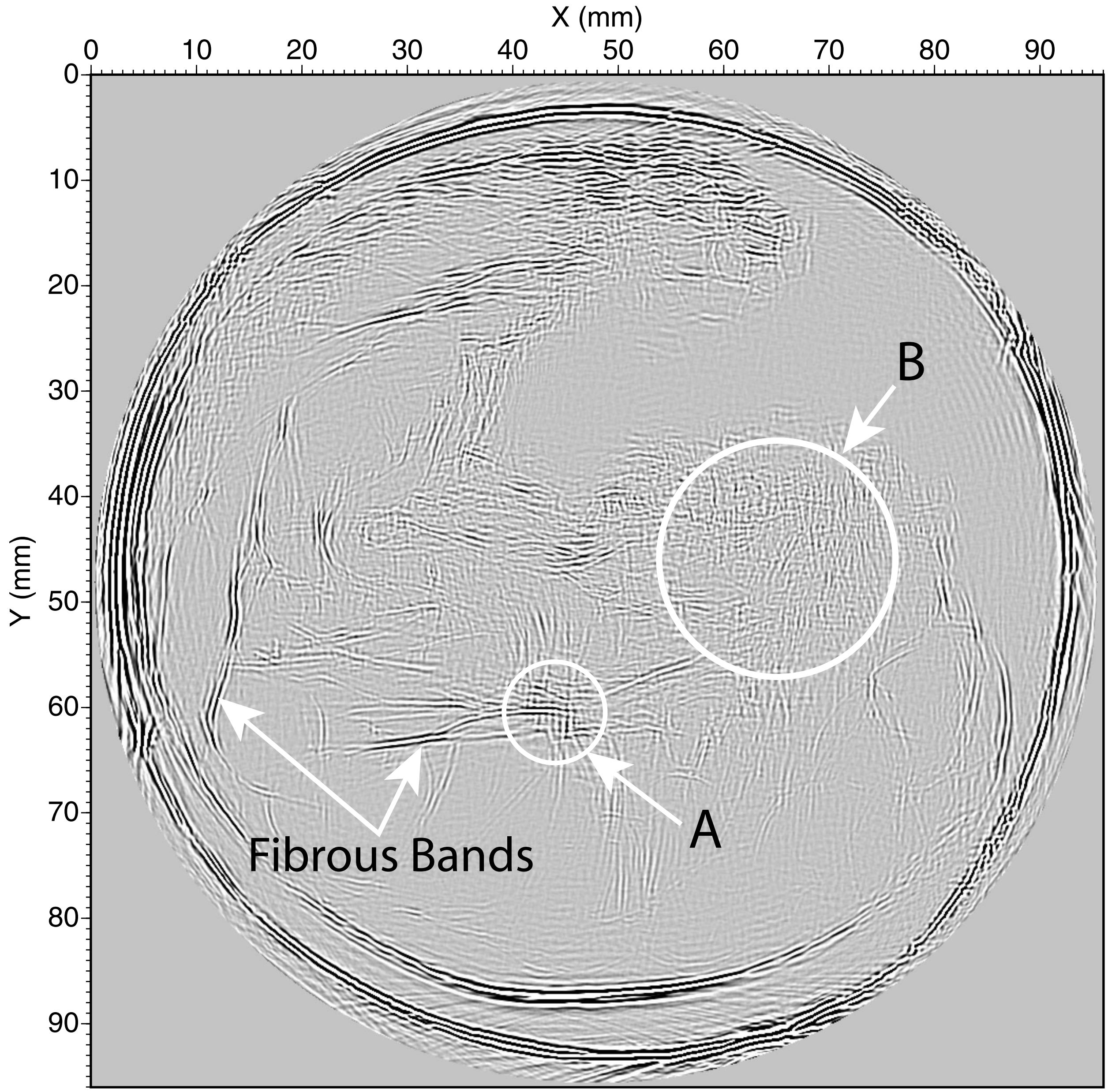

Figure 7. Image obtained using wave-based reflection imaging for the breast specimen. The fibrous bands and complex structure in region A can also be seen in the x-ray CT image shown in Figure 8. The images around region B are not clear and need to be improved using an ultrasonic imaging method capable of handling the heterogeneous nature of breast tissue.

specimen obtained using our wave-based imaging method. It shows clear images of fibrous bands and complex structure in region A. The breast specimen was also scanned with a clinical x-ray CT scanner (GE Lightspeed Quad detector array). This was used to establish the "truth" images. It shows the x-ray attenuation of tissue in the breast specimen. The x-ray CT scans were perform at 1.25-mm slice thickness. Figure 8 is a stacked image of 8 slices of the x-ray CT images, and hence, it represents the image of a slice having the same thickness as that for ultrasonic imaging. The corresponding breast structures shown in Figure 7 can also be seen in Figure 8.

It is obvious that the x-ray CT image has much higher resolution than x-ray mammogram. However, this x-ray CT scanning was conducted for the cadaveric breast specimen, and clinical imaging does not use x-ray CT scanning for the

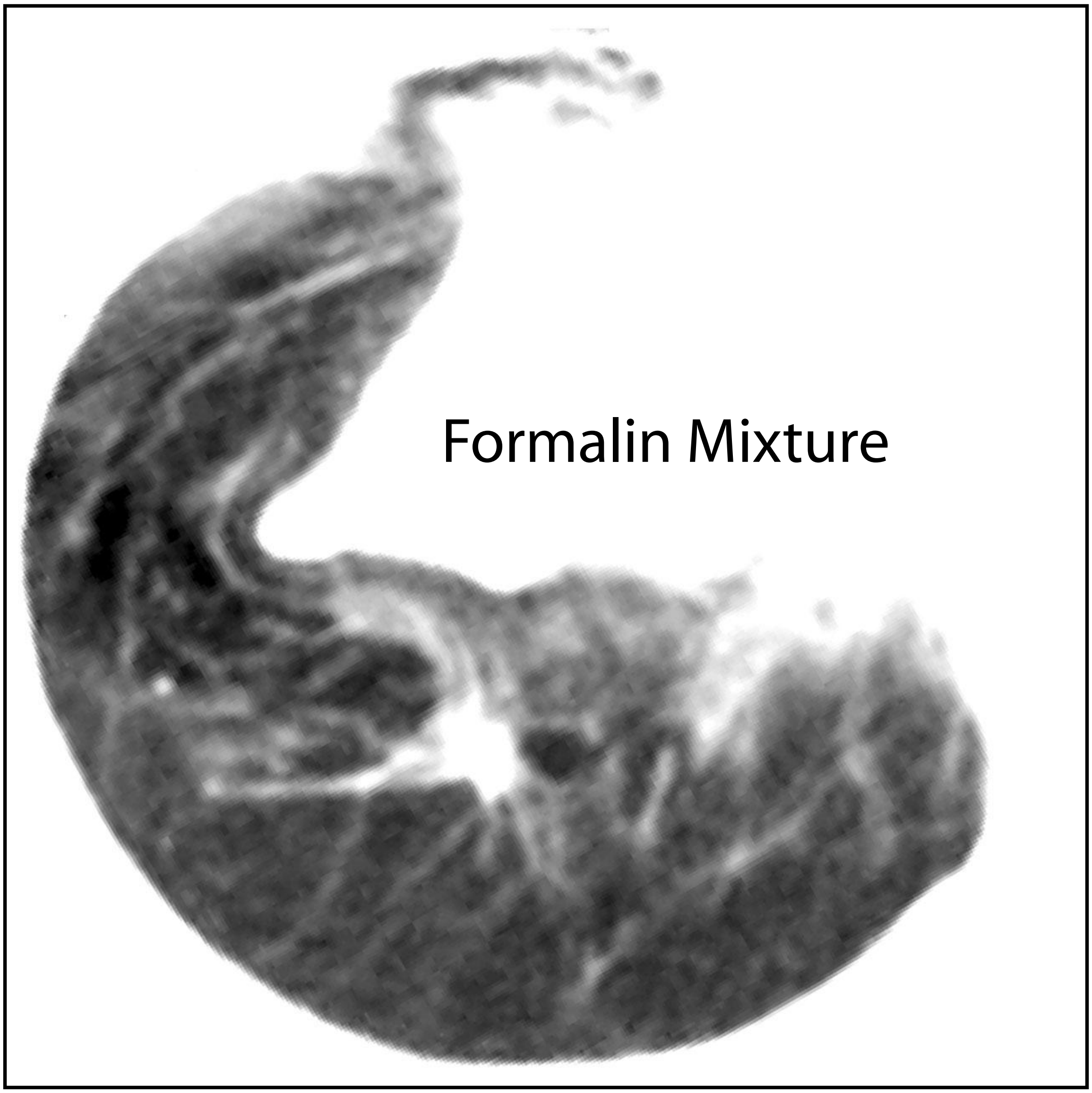

Figure 8. An x-ray CT (computed tomography) image of the breast specimen shows x-ray attenuation of the breast tissue.

breast because of dangers of strong ionizing radiation.

The larger area of formalin mixture in Figure 8 than that in Figure 7 is because the cylindrical tube containing the breast specimen was laid down during the x-ray CT scanning and stood up during the ultrasonic scanning.

We note that some regions of Figure 7, such as those around the circle at location B, are not clear. This demonstrates that it is essential to develop wave-based ultrasonic imaging methods capable of handling the heterogeneous nature of breast tissue to produce clear and accurate breast images, because the sound speeds of breast tissue could vary approximately from 1400 m/s to 1600 m/s. We will report in the near future on imaging results using reflection imaging methods based on solutions of the acoustic-wave equation in heterogeneous media.

We believe that the new KCI ultrasonic breast-scanning device coupled with new imaging methods capable of handling heterogeneous nature of breast tissue could vastly improve the capability of ultrasonic breast imaging. This could eventually provide a safe (non-ionizing radiation), cheap, portable, and essential new tool for early detection and diagnosis of breast cancer.

5. CONCLUSIONS

We have introduced a new ultrasonic reflection imaging method using the solution of the wave equation in a constant-velocity medium. Fast Fourier Transform algorithms are used during numerical implementation to improve the computational efficiency of imaging. In the new imaging method, a range of frequency of interest can be selected and the effects of ultrasonic-wave attenuation could be compensated approximately during imaging to produce more realistic breast images. Our preliminary imaging results demonstrate that the new reflection imaging method has the potential to produce high-resolution images showing detailed structures of the breast. Ultimately, an ultrasonic imaging method based on solutions of the wave equation in heterogeneous media is required to accurately account for effects of the heterogeneous nature of breast tissue.

ACKNOWLEDGMENTS

This research was supported by the United States Department of Energy through contract W-7405-ENG-36 to Los Alamos National Laboratory (LANL). We thank Kenneth Hanson at LANL and Michael Insana at the University of California at Davis for their valuable comments and suggestions, and George Randall at LANL for the helpful discussion on deconvolution. Lianjie Huang greatly appreciates the support and encouragement from Michael Fehler at LANL. We thank the Karmanos Cancer Institute for its permission to release the ultrasonic imaging results.

REFERENCES

1. P. C. Gotzsche and O. Olsen, "Is screening for breast cancer with mammography justifiable?," *The Lancet* **355**, pp. 129–134, 2000.
2. O. Olsen and P. C. Gotzsche, "Cochrane review on screening for breast cancer with mammography," *The Lancet* **358**, pp. 1340–1342, 2001.
3. E. A. Sickles, "Breast imaging: From 1965 to the present," *Radiology* **215**, pp. 1–16, 2000.
4. S. J. Nass, I. C. Henderson, and J. C. Lashof (National Cancer Policy Board), eds., *Mammography and Beyond: Developing Technologies for the Early Detection of Breast Cancer*, National Academy Press, 2001.
5. T. M. Kolb, J. Lichy, and J. H. Newhouse, "Occult cancer in women with dense breast: detection with screening us diagnostic yield and tumor characteristics," *Radiology* **207**, pp. 191–199, 1998.
6. J. R. Parikh and B. Porter, "Understanding breast ultrasound," *Imaging Economics (The Journal of Imaging Technology Management)* (2002 March issue), pp. 16–20,32, 2002.
7. A. T. Stavros, D. Thickman, C. L. Rapp, M. A. Dennis, S. H. Parker, and G. A. Sisney, "Solid breast nodules: use of sonography to distinguish between benign and malignant lesions," *Radiology* **196**, pp. 113–134, 1995.
8. H. M. Zonderland, E. M. Coerkamp, J. Hermans, M. J. van de Vijver, and A. E. van Voorthuisen, "Diagnosis of breast cancer: Contribution of US as an adjunct to mammography," *Radiology* **213**, pp. 413–422, 1999.
9. P. Littrup, et al., "Computerized Ultradound Risk Evaluation (CURE) system: Development of combined transmission and reflection ultrasound with new reconstruction algorithms for breast imaging," *Acoustic Imaging* **26**, pp. 175–182, 2002.
10. P. Littrup, N. Duric, R. R. Leach Jr., S. G. Azevedo, J. V. Candy, T. Moore, D. H. Chambers, J. E. Mast, and E. T. Holsapple, "Characterizing tissue with acoustic parameters derived from ultrasound data," in *Ultrasonic Imaging and Signal Proceesing*, M. Insana and W. F. Walker, eds., *Proc. SPIE* **4687**, pp. 354–361, The International Society for Optical Engineering, (Bellingham, Washington), 2002.
11. N. Duric, P. Littrup, E. T. Holsapple, A. Babkin, R. Duncan, A. Kalinin, R. Pevzner, and M. Tokarev, "Ultrasound tomography of breast tissue," in *Ultrasonic Imaging and Signal Processing*, W. F. Walker and M. Insana, eds., *Proc. SPIE* **5035**, The International Society for Optical Engineering, (Bellingham, Washington), 2003.
12. R. R. Leach Jr., S. G. Azevedo, J. G. Berryman, H. R. Bertete-Aguirre, S. H. Chambers, J. E. Mast, P. Littrup, N. Duric, S. A. Johnson, and F. Wuebbeling, "Comparison of ultrasound tomography methods in circular geometry," in *Ultrasonic Imaging and Signal Proceesing*, M. Insana and W. F. Walker, eds., *Proc. SPIE* **4687**, pp. 362–377, The International Society for Optical Engineering, (Bellingham, Washington), 2002.
13. D. H. Chambers and P. Littrup, "Ultrasound imaging using diffraction tomography in a cylindrical geometry," in *Ultrasonic Imaging and Signal Processing*, M. Insana and W. F. Walker, eds., *Proc. SPIE* **4687**, pp. 412–420, The International Society for Optical Engineering, (Bellingham, Washington), 2002.